DEUTSCHES ELEKTRONEN-SYNCHROTRON DESY

DESY SR 84-13
April 1984

DETECTION OF DEFECT-FREE ZONES IN ANNEALED CZOCHRALSKI SILICON WITH SYNCHROTRON SECTION TOPOGRAPHY

by

T.Tuomi

Lab. of Physics, Helsinki Univ. of Technology, Espoo

M. Tilli

Lab. of Phys. Metallurgy, Helsinki Univ. of Technology, Espoo

O. Antilla

Semiconductor Lab., Technical Research Centre of Finland, Espoo

NOTKESTRASSE 85 · 2 HAMBURG 52

DESY SR 84-12
April 1984

ISSN 0723-7979

DETECTION OF DEFECT-FREE ZONES IN ANNEALED CZOCHRALSKI SILICON WITH SYNCHROTRON SECTION TOPOGRAPHY

T. Tuomi (a), M. Tilli (b) and O. Anttila (c)

(a) Laboratory of Physics, Helsinki University of Technology
SF-02150 Espoo, Finland
(b) Laboratory of Physical Metallurgy, Helsinki University of
Technology, SF-02150 Espoo, Finland
(c) Semiconductor Laboratory, Technical Research Centre of
Finland, SF-02150 Espoo, Finland

Abstract

High-resolution, rapid synchrotron x-ray topography is used to study oxygen-induced microdefects and their spatial distribution in a large number of (100) n-type silicon wafers, which had undergone different two-stage thermal anneals. Section topographs reveal a 40 to 60 μm-thick defect-free zone on the surface of a wafer annealed first at 800 °C for 20 h and then at 1150 °C for 4 h.

ISSN 0723 - 7979

Dislocation-free silicon crystals grown by the Czochralski technique contain 5×10^{17} to 10^{18} atoms/cm^3 of interstitial oxygen. In post-growth thermal treatments oxygen tends to precipitate and stacking faults are also formed. Because these microdefects are deleterious to integrated circuits it is tried to avoid them as much as possible. Although the total removement of the oxygen or oxygen-associated microdefects is not reasonable, a defect-free zone near the surface of a wafer can be made with heat treatments /1/. Moreover, the defects left in the interior of the wafer act as gettering centres for unwanted impurities /2/.

It is important to develop non-destructive and rapid techniques for detection and measurements of the defect-free zone in order to improve processes which results in the best possible wafers for microelectronics industry. X-ray section topography /3/ is such an imaging technique especially when synchrotron radiation is used. High-resolution topographs are made with synchrotron radiation in seconds /4/.

The silicon wafers 75 mm (3 in) in diameter were grown by the Czochralski technique at a pulling rate of 1.4 to 1.5 mm/min. They were polished both sides with the standard chemical-mechanical method to a thickness of 380 ± 10 μm. The wafers were n-type and their resistivity ranged from 5 to 6 Ωcm. The oxygen concentration was 17.5 to 18 ppm measured with a double-beam infrared spectrometer according to the ASTM F121-80 standard.

A two-step heat treatment of the wafers, from which results are presented in this work, consisted of an anneal at 800 °C in nitrogen for 20 h followed by heating to 1150 °C also in nitrogen for 4 h. The wafers were then steam oxidized at 1100 °C for 2 h. The oxide layer was removed with hydrofluoric acid.

The synchrotron x-ray topographs were made at the topography station of the Hamburger Synchrotronstrahlungslabor (HASYLAB) using spectrally continuous radiation from the DORIS electron-positron ring. The electron energy was 3.685 GeV and the current 60 to 80 mA. The flux of a beam diffracted from a perfect silicon crystal was about 10^7 photons s^{-1} mm^{-2}

per $\Delta E/E = 10^{-5}$ bandwidth at the x-ray photon energy E = 12 keV.

The topographs were made on Kodak High Resolution films whose grain size was of the order of 0.05 μm. Although the synchrotron radiation had a very high intensity, the films had to be exposed for 1 to 2 min when making a Laue set of large area (5 x 5 mm^2) transmission topographs and for at least 5 to 10 min when a similar set of section topographs was recorded.

The (100)-surface of the silicon single crystal wafer made an angle of 18.2° with the incident beam. The <011> direction was only approximately vertical so that multiple diffraction did not occur. The film was placed perpendicularly to the incident beam 48 mm behind the sample for making large-area transmission topographs. The section topographs were made with a narrow slit formed by two parallel vertical polished tungsten rods having a diameter of 2 mm. The width of the slit measured from a red image on an exposed radiation sensitive paper was 25 to 65 μm. In section topography the film was parallel to the silicon wafer 48 mm from it.

The spatial resolution estimated from the size of the synchrotron radiation source, from the source-to-film distance and from that between the sample and the source, was about 5 μm.

In this work results are presented on a sample which had undergone a 800 °C anneal followed by a 1150 °C heat treatment and a steam oxidation at 1100 °C. However, altogether some 50 wafers were examined with synchrotron radiation. The wafers had been heat treated at different high temperatures between 1100 °C and 1250 °C for 6 to 1 hours in nitrogen. Before or after this they were kept at 725 °C or 800 °C for 20 h. After the two-step anneal most wafers were steam oxidized at 1100 °C for 2 h. However, a few samples were left unoxidized for comparison. For the same reason some wafers were annealed only once either at the low or high temperature.

During the first step of the anneal (at 800 °C) interstitial oxygen is thought to begin to precipitate and oxide is formed. The subsequent

high temperature anneal (at 1150 °C) is intended for the outdiffusion of oxygen from the surface layer, the thickness of which is equal to the diffusion length (at 1150 °C). In addition the small precipitates or clusters already formed during the nucleation step of the anneal begin to dissolve. The stable nuclei also formed during the first step of anneal grow in size and may often develop to stacking faults.

Figure 1 shows a $\bar{4}00$ transmission topographs of the silicon wafer. The density of the microdefects is so large that the images of individual defects overlap and therefore their details are not well discernable. The contrast of the microdefects was rather different in other topographs such as $\bar{1}31$, $3\bar{1}1$, $0\bar{4}0$ and 111, all of which were made at the same time on the same film. However, none of them showed the defects in detail.

Figure 2 shows a $\bar{2}\bar{2}0$ section topograph of the same sample. The microdefects are seen as rather well separated spots having a diameter of about 10 μm in the central stripe of the topograph. At the edges there are no defect images.

In an x-ray topograph the image of a defect can be direct, intermediary or dynamical depending on the absorption of the smaple. Direct images are black, i.e. there is an enhanced radiation intensity which blackens the film. Dynamical images may be described as shadows cast by the defect and therefore they have a white centre. The spots seen in Fig. 2 are all black direct images of microdefects. They are formed by the direct beam diffracted from the defect and from the misoriented and strained region surrounding it.

The principal x-ray wavelengths contributing to the image of this $\bar{2}\bar{2}0$ topograph are 60 pm and 40 pm. For these reflections ($\bar{4}\bar{4}0$ and $\bar{6}\bar{6}0$) the absorption coefficient times the thickness of the sample (in the direction of the direct beam) is $\mu t \approx$ 0.1 to 0.3. The minor contributions to the diffracted beam from the fundamental (λ_1 = 120 pm) and the other harmonics can be calculated as shown in Ref. 4. Pendellösung fringes are not seen in the section topograph, because the two sets of fringes produced by the two wavelengths overlap and because the defect image density is large. Still another reason for the disappearance of the Pendellösung fringes is the finite width of the narrow beam.

Figure 3 shows schematicly how a section topograph is made with the narrow ribbon-like direct beam and how the cross-section of the sample is imaged. With the aid of Fig. 3 the depth of a defect-free zone can be calculated from the width w of the spotless stripe visible on both edges of the section topograph. In the wafer whose section topograph is shown in Fig. 2 the thickness of the defect-free zone or surface layer is $w' = 40$ to 60 μm measured from the topograph. It is worth noticing that the finite slit width widens the section topograph from the ideal picture of Fig. 3. The width of the spotless stripe w does not, however, change. Etching in Wright-etch revealed a defect-free zone of 40 to 60 μm thick, too. The diffusion length of interstitial oxygen is, however, only 15 to 20 μm according to the measured diffusiveness. This discrepancy may be due to the effect of stresses near the surface and the effect of intrinsic point defect concentrations to the formation of oxide precipitates.

The section topographic method may be used in detecting defects such as oxygen-induced precipitation and stacking faults in the course of wafer processing. The imaging technique is non-destructive and rapid enough so that a large number of wafers can be examined in reasonable times. It is also possible to proceed the process after the wafers have been examined.

This work is supported by the silicon wafer research consortium formed by Helsinki University of Technology, Nokia Corporation Electronics, and Outokumpu Oy which is gratefully acknowledged.

The heat treatments were made at the Semiconductor Laboratory, Technical Research Centre of Finland, as a part of the Semiconductor Technology Development Program.

The authors also want to thank Professor C. Kunz for permission to use the synchrotron radiation facility at the HASYLAB, Hamburg, and Dr. W. Graeff for help at the topography station.

References

1. H. Richter, M. Mai, F.-G. Kirscht and P. Gaworzewski, Physica 116B, 162 (1983)
2. T. Y. Tan, E. E. Gardner and W. K. Tice, Appl. Phys. Lett. 30, 175 (1977)
3. A. R. Lang, Acta Met. 5, 358 (1957)
4. T. Tuomi, K. Naukkarinen, E. Laurila and P. Rabe, Acta Polytechnica Scand. Ph100, 1 (1973) and T. Tuomi, K. Naukkarinen and P. Rabe, phys. stat. sol. (a) 25, 93 (1974)
5. U. Gösele and T. Y. Tan, Appl. Phys. A28, 79 (1982)

Captions of figures

Fig. 1. $\bar{4}00$ transmission synchrotron x-ray topograph of a thermally annealed Czochralski grown (100)-silicon wafer.

Fig. 2. $n(\bar{2}\bar{2}0)$ synchrotron section topograph of the same thermally annealed Czochralski grown (100)-silicon wafer as in Fig. 1.

Fig. 3. Schematic illustration of (direct) image formation in section topography. S sample, f film, i section topograph, ω and ω' width of a defect-free zone on the topograph and in the sample.

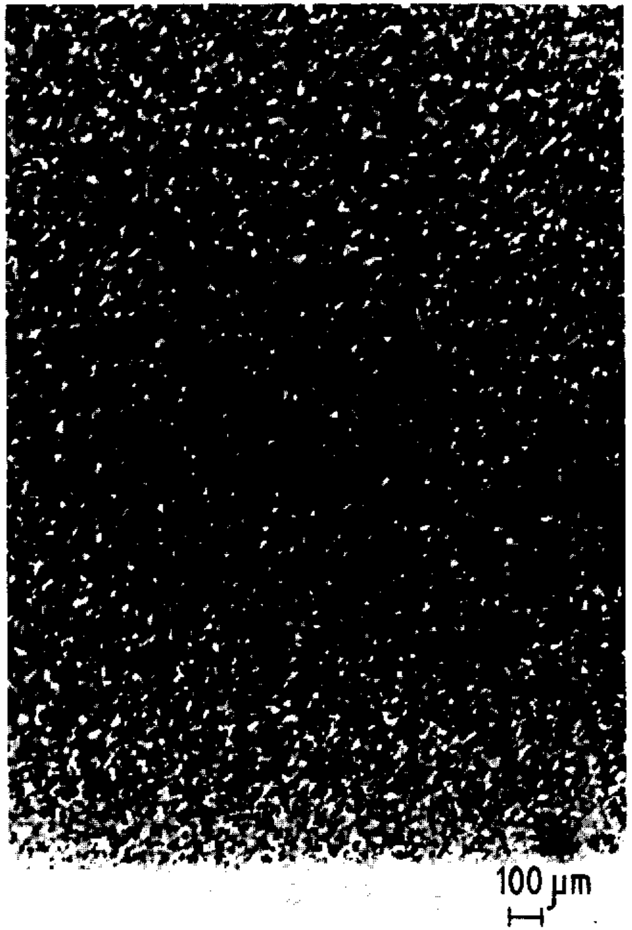

Fig. 1

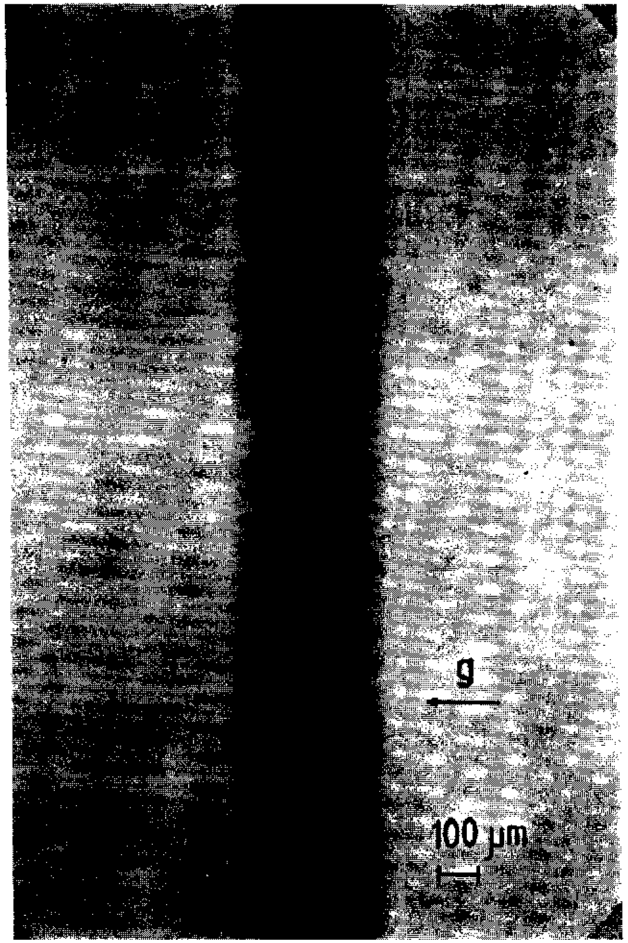

Fig. 2

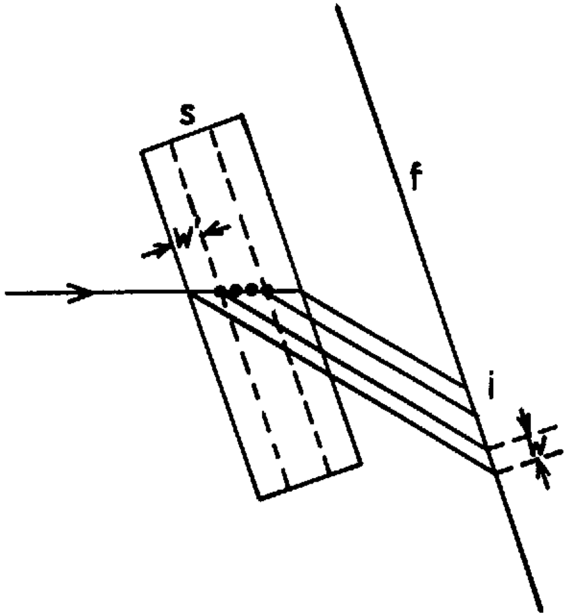

Fig. 3